Heat Transfer / Film Cooling
Paper 23

THE TRANSIENT LIQUID CRYSTAL TECHNIQUE APPLIED FOR INVESTIGATIONS OF FLAT PLATE AND SHOWERHEAD FILM COOLING.

U. Drost, A. Bölcs

Laboratoire de Thermique appliquée et de Turbomachines (LTT)
Swiss Federal Institute of Technology
CH-1015 Lausanne

The Transient Liquid Crystal Technique Applied for Investigations of Flat Plate and Showerhead Film Cooling

U. Drost, A. Bölcs

Laboratoire de thermique appliquée et de turbomachines
EPF-Lausanne

ABSTRACT

The transient liquid crystal technique has been employed for film cooling measurements on a flat plate and a cylinder geometry, conducted in a free jet test facility.

The experimental setup and the methods employed to derive the film cooling properties are presented. Measurement results for a flat plate with a single row of 35° inclined holes, as well as stagnation point cooling results for a cylinder with a four cooling row configuration, are shown to illustrate the measurement technique. Engine representative conditions are simulated in terms of Reynolds, Mach number and density ratio, using foreign gas injection.

LIST OF SYMBOLS

c_p specific heat capacity [J/kgK]
d cooling hole diameter [mm]
DR density ratio ρ_c/ρ_g
G blowing ratio $\rho_c u_c/\rho_g u_g$
I momentum flux ratio $\rho_c u_c^2/\rho_g u_g^2$
l_h hole length [mm]
l_p hole pitch [mm]
p pressure [Pa]
q surface heat flux [W/m²]
ρ density [kg/m³]
T temperature [K]
u velocity [m/s]
x axial coordinate [mm]

Greek

α convective heat transfer coefficient [W/(m²K)]
η film cooling effectiveness $(T_{aw}-T_{rg})/(T_{tc}-T_{tg})$
τ measurement time [s]
λ thermal conductivity [J/mK]
Λ thermal diffusity ($\lambda/\rho c_p$) [m²/s]

Indices

aw adiabatic wall
c coolant
g freestream
i initial
r recovery
t total
w wall
∞ infinite

Dimensionless Numbers

Nu Nusselt number ($\alpha L/\lambda_{fluid}$)
Pr Prandtl number ($c_p \mu/\lambda$)
Re Reynolds number (uL/ν)

INTRODUCTION

The power output and efficiency level of a gas turbine improves by increasing the turbine inlet temperatures. Since these temperatures exceed the highest allowable blade material temperature the blades have to be cooled to guarantee safe operating conditions and reasonable life time. Discrete hole film cooling is an effective way to achieve this objective, provided that the thermal boundary conditions are accurately known. As numerical predictions of three-temperature convection situations on complex geometries as turbine airfoils are not yet sufficiently reliable for design purposes experimental information is urgently needed.

In the present work, an evaluation procedure is presented allowing the deduction of both the film cooling effectiveness and heat transfer coefficients from multiple transient tests conducted at identical aerodynamic, but varying coolant injection temperatures. This evaluation procedure has been applied to measurements on a flat plate with a single cooling hole row and a cylinder model with four staggered cooling hole rows in the stagnation region, simulating showerhead cooling of a turbine airfoil.

Theory

The local heat flux in the film cooling situation can be described as follows,

$$q = \alpha_f (T_{aw} - T_w) \tag{1}$$

where the convection coefficient is based on the unknown adiabatic wall temperature that depends on the supply temperatures of the main and secondary streams and the degree of mixing. In dimensionless form this temperature becomes the film cooling effectiveness, defined as (Teekaram et al., 1990),

$$\eta = \frac{T_{aw} - T_{rg}}{T_{tc} - T_{tg}} \tag{2}$$

The two unknowns of such a three-temperature situation are thus the heat transfer coefficient α_f and the film cooling effectiveness, η. Both values are functions of the aerodynamic character of the flow field alone (Vedula and Metzger, 1991).

In the present work, these two unknowns are determined by conducting transient tests where the model is suddenly exposed to a steady mainstream. The transient heating of the surface is monitored by the color play of a liquid crystal coating. Initially the model is at a homogenous temperature, so that for short testing times the transient heating near the surface can be described by one-dimensional semi-infinite heat conduction. The governing differential equation and appropriate boundary conditions are then,

$$\frac{\partial^2 T}{\partial x^2} = \frac{1}{\Lambda} \frac{\partial T}{\partial t} \tag{3}$$

$$\lim_{x\to\infty} T(x,t) = T_i \tag{4}$$

$$T(x,0) = T_i \tag{5}$$

$$-\lambda \frac{\partial T(0,t)}{\partial x} = \alpha_f \left(T_{aw} - T(0,t)\right) \tag{6}$$

In the experiments a complication is introduced, since a true step change of the coolant temperature is not possible due to heat exchange in the supply tubing and plenum chamber. Thus, the adiabatic wall temperature becomes a function of time, which has to be accounted for in the evaluation. Hence, the measured coolant temperature distribution is approximated by a power series of the following form,

$$T_{tc}(t) = \sum_{n=0}^{N} A_n \frac{t^n}{\Gamma(n+1)} \tag{7}$$

usually chosen of 4th to 5th order (Fig. 1).

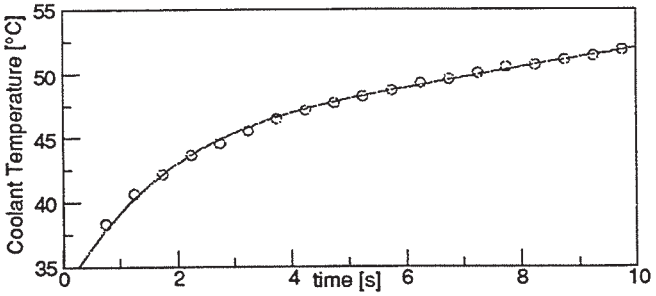

Figure 1 *Coolant temperature evolution and 5th order fit*

Using this closed expression for T_{tc}, an analytical solution to the equations (3) to (7) is obtained using the Laplace transform method,

$$\begin{aligned} T_w - T_i = {} & \left(T_{rg} - \eta T_{tg} - T_i\right)\left[1 - e^{\beta^2}\,\mathrm{erfc}(\beta)\right] \\ & - \eta \sum_{n=0}^{N} \left\{ A_n \left(\frac{\kappa}{\alpha_f}\right)^{2n} \left[e^{\beta^2}\,\mathrm{erfc}(\beta) - \sum_{\tau=0}^{2n} \left([-2\beta]^{\tau} i^{\tau}\,\mathrm{erfc}(0) \right) \right] \right\} \end{aligned} \tag{8}$$

with

$$\kappa = \frac{\lambda}{\sqrt{\Lambda}} = \sqrt{\rho \cdot \lambda \cdot c_p}$$

$$\beta = \frac{\alpha_f \sqrt{t}}{\kappa}$$

Eq. (8) contains the two unknowns α_f and η, which are deduced via a regression analysis similar to that proposed by Wang et al. (1994). Least

squares fitting of the model equation to the wall temperature rise yields the two unknowns. Wang measured the wall temperature during a single experiment with large-band liquid crystals. In theory two points of the temperature history would be sufficient to determine the two unknowns at each point of the surface. However, the measurement uncertainty can be significantly reduced by adding additional points to the evaluation and by applying regression analysis.

In the present work, a single layer of narrow-band liquid crystal is used to avoid additional complications related to the view angle dependency of large-band liquid crystals. Multiple layers of narrow-band liquid crystals can not be employed, because the hue signals recorded by the image processing system does not allow a clear identification of each layer.

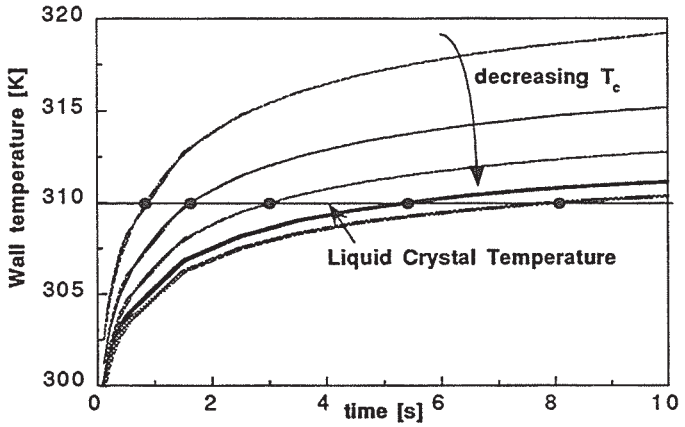

***Figure 2** Multiple test regression analysis*

For the present study usually 6 to 8 tests were carried out at identical blowing ratios, total temperatures and liquid crystal temperatures, whereas the coolant injection temperature was varied (Fig. 2). These test ensembles were then evaluated together by fitting eq. (8) through the measured points using a least squares regression procedure.

TEST FACILITY

The measurements were conducted in a free jet test facility with a nozzle diameter of 150 mm as shown in Fig. 3. The test facility is supplied from a continuously running air source delivering a mass flow up to 10 kg/s with a maximum pressure ratio of 3.5.

In order to obtain a high turbulence level, a square array biplane grid constructed with rectangular bars has been inserted. The turbulence grid has a meshsize of 15 mm, a mesh- to barsize ratio of 5, and is placed 8.5 meshsizes upstream of the injection location on the flat plate or 10 meshsizes from the cylinder leading edge, respectively, to achieve nearly isotropic turbulence following the recommendations of Baines and Peterson (1951).

The turbulence intensity decay downstream of the grid yields 15% at the upstream border of the flat plate and 8 % at the injection location. At the leading edge location of the film cooled cylinder, the Tu intensity is 7%. Length scale growth was weak yielding a length scale of about 9 mm at the injection locations.

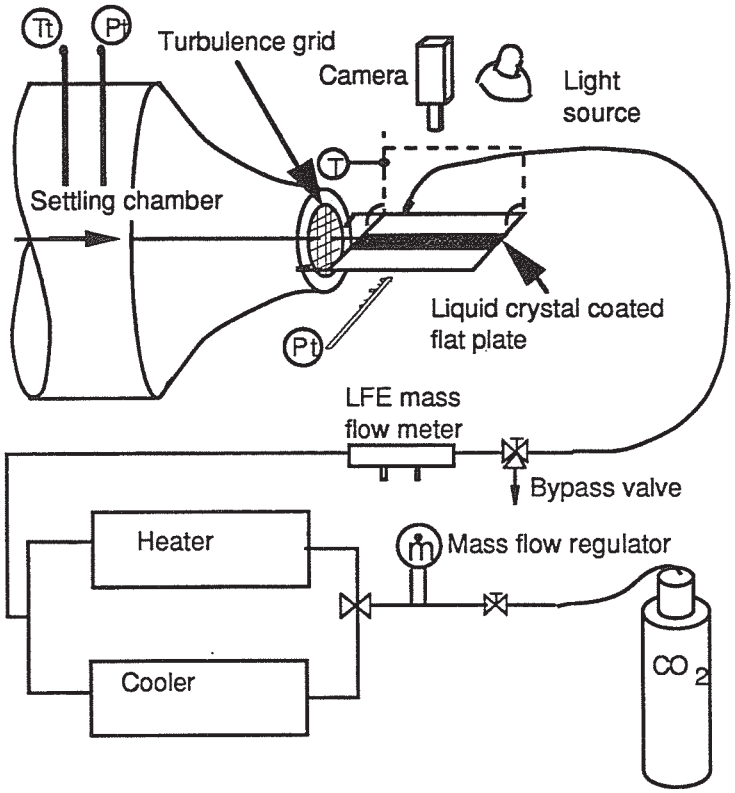

Figure 3 *Free jet test facility with grid*

Flat Plate Model

Transient experiments on the flat plate in the free jet test facility are conducted using an insertion device where the plate is pivoted about a shaft parallel to the flow direction (Fig. 4). The initial temperature of the plate is allowed to stabilize in a vertical position outside of the jet before the plate is rapidly exposed to the flow. The leading edge of the plate has a semi-elliptic profile shape of ratio 4:1 to ensure the development of a laminar boundary layer.

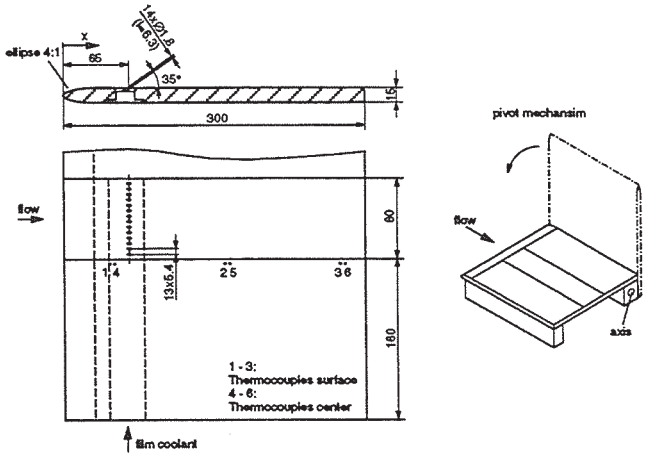

Figure 4 *Flat plate for film cooling measurements*

The film cooling geometry consists of one row of 14 holes with diameter d=1.8 mm inclined with 35° in the flow direction from the surface. The ratio of hole spacing to diameter is 3, and the ratio of the injection hole length to diameter is

3.5. The injection system has a feeding chamber in the model itself and supply of the coolant from one side similar to a blade. The internal walls of the film coolant supply are insulated with balsa wood to minimize heat exchange. The coolant properties are measured in the plenum chamber with two thin-foil thermocouples on small perspex supports and a static pressure tapping.

Cylinder Model

For cylinder measurements, a similar insertion system as for the flat plate has been developed, however with the possibility to precool the measurement section of the cylinder to increase the wall to mainstream temperature difference. The cylinder is fixed on a shaft and pivoted rapidly into the flow once initial conditions have been established (Fig. 5).
Static pressure tappings are placed over about 180° besides the measurement region. Two transient thermocouples and a static pressure tapping are located in the coolant plenum behind the coolant holes, while a fine gauze is installed upstream to increase the fluid mixing. A flexible tube with a heat exchanger is used to connect the coolant supply and the bypass valve.

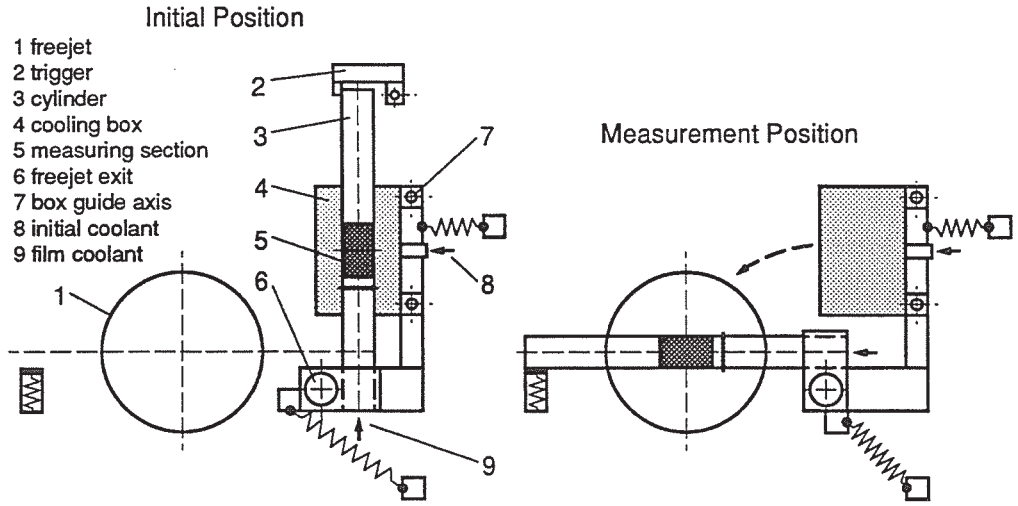

Figure 5 *Cylinder insertion and measurement system*

The actual showerhead cooling geometry consists of a four-row configuration in staggered arrangement (Fig. 6).

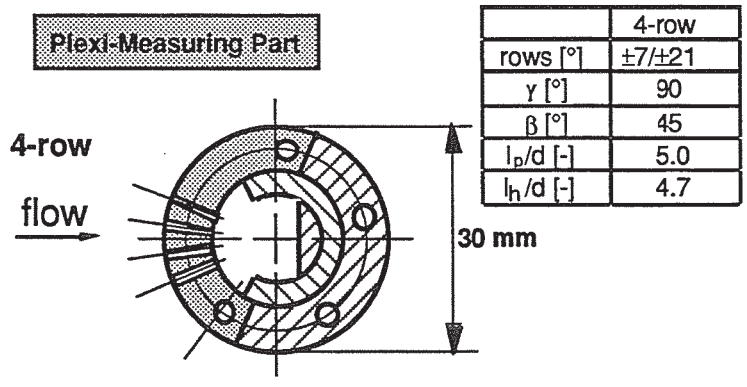

	4-row
rows [°]	±7/±21
γ [°]	90
β [°]	45
l_p/d [-]	5.0
l_h/d [-]	4.7

Figure 6 *Cylinder model for showerhead cooling*

MEASUREMENT EQUIPMENT

Various physical quantities must be measured to deduce the film cooling heat transfer coefficient and effectiveness according to equations (1) and (2).
In terms of mainstream properties, the total temperature and surface pressure distribution must be known to obtain the local recovery temperatures which appear in the film cooling effectiveness definition, as well as the local density and velocity at the injection locations in order to calculate the blowing and momentum flux ratios.
In regard to the coolant properties, the coolant mass flow rate, temperature and pressure must be quantified at the injection locations, hence the cooling hole exists. Since measurements at the exits are impossible they are carried out in the coolant plenum chamber close to the hole entries assuming an adiabatic expansion of the coolant flow from the hole entry to the exit.
The pressures are determined with an automated acquisition system. A total of 192 pressures can be measured with four pressure sensors (Digiquarz 2100 AT, 0-6.9 bar, precision 0.01% full scale) in combination with a scanner (Scanivalve 48364 GM-1). For low velocities a high precision differential pressure sensor (Digiquarz 1003D-01, 0-180 mbar, precision 0.01% full scale) is used. Additional differential pressure devices are taken for coolant massflow determination and plenum pressure measurement (Effa SK, 0-25 or 0-800 mbar, precision 0.2%).
Temperatures are measured with K type thermocouples. They can be calibrated very precisely (better than 0.1 K) and are small enough to be incorporated into models and aerodynamic probes. The reference junction are immersed in an electronically controlled ice bath and the micro-voltages are measured with a precision multimeter which can operate in steady-state or transient mode (Hewlett Packard 75000).
The massflow meter used to determine the coolant massflow is a Laminar Flow Element (LFE) from Meriam Instruments Ltd., Ohio, based on the laminar Hagen-Poiseuille flow in a tube. As accurate measurement of the coolant massflow is essential for the determination of the film cooling parameters a second massflow meter is used in serie for additional control and regulation (Brooks type 5853S). This meter is also used for the adjustment of the coolant parameters as it allows the mass flow rate regulation via a fast reacting valve controlled by a PID regulator.

Coolant conditioning and bypass system

A cooling system is dimensioned and designed to supply the cooling air for the initial conditioning of the models and the film coolant. The main unit is a cryostat (Lauda RUK90-W) with 0.9 kW cooling power at a bath temperature of -60°C. Two corrugated plate heat exchangers allow a constant cooling of 300 stl/min of initial cooling air and 300 stl/min of film coolant (air or CO_2) to a temperature of -50 °C. The cooling air is taken from a pressurized air system at 8 bar with a dew point of around 0 °C. Thus, an additional air dryer with two absorption chambers (Zander CPQ-KEN-150) is used to avoid icing in the heat exchangers. Since the heat exchangers are always supplied with the same cooling bath temperature both lines are equipped with a bypass for an independent regulation of the desired temperatures. As the film coolant also

needs to be above ambient temperature a heating bath was added for this purpose.

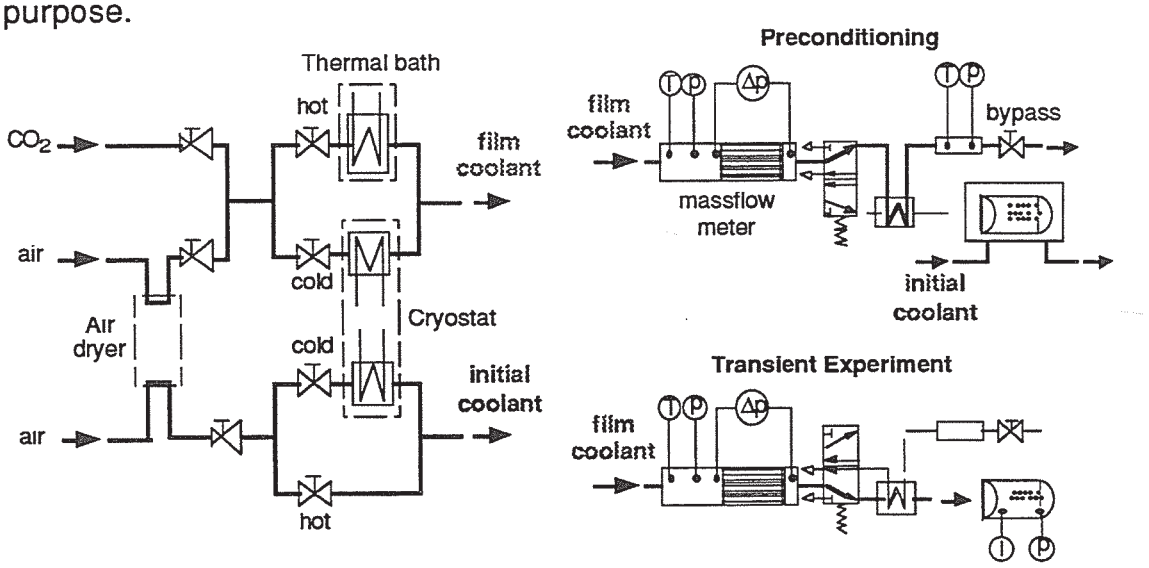

Figure 7 *Coolant conditioning system*

The film coolant and its circuit have to be preconditioned via a bypass before the transient experiment starts (Fig. 7). The counterpressure in the bypass is adjusted according to the actual test conditions to avoid flow oscillations when the valve is triggered.

Image Processing

The tests are conducted with a sophisticated automated image processing system (Vitronic GmbH, Germany) which is based on the hue capturing (or surface color) technique. Complete liquid crystal image sequences are taken in real time at the conventional video frame rate of 25 Hz, but only pre-selected hue values are stored in the random access memory of the computer. If these values do not exceed about 30% of the complete image, a full transient experiment can be recorded up to approximately 30 seconds.

The image aquisition and processing is explained in Fig. 8. Before a transient test serie, a color grid is recorded with the image processing system. The grid data is then transmitted to an HP workstation, and, using spline curve interpolation, a coordinate transform from pixel to surface coordinates is carried out.

Transient experiments are recorded with a CCD camera and transferred to the image processing system. The complete images are immediately filtered and only preselected color values are retained. After testing, the image data files are transmitted to the workstation and the previously performed coordinate transform is applied to the image sequences. Subsequently, data reduction is carried out.

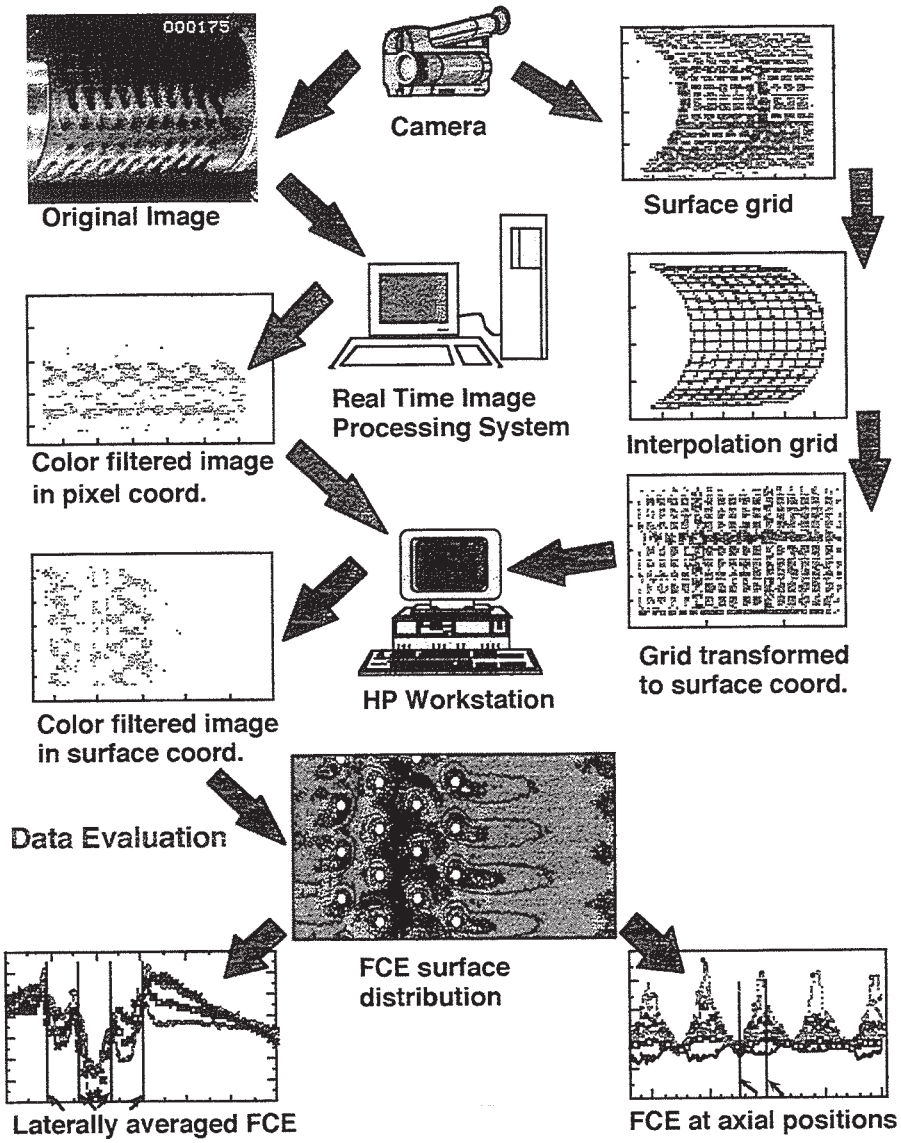

Figure 8 *Image processing system*

RESULTS

Flat Plate

The complete surface effectiveness distributions were integrated over 27 mm in the flow center to obtain laterally averaged values $\overline{\eta}$. Fig. 9 shows the evolution of $\overline{\eta}$ for different blowing ratios at a Mach number of 0.3. For low blowing ratios $\overline{\eta}$ has a maximum near the holes and monotonically decreases further downstream. Jet lift-off occurs at a blowing rate of about 1, which flattens the effectiveness in vicinity to the holes, but produces rather high values further downstream. Highest overall effectiveness is observed at G=0.7.

The excellent resolution of the measurements, considering the small hole diameter of 1.8 mm, is illustrated by spanwise effectiveness distributions at different axial positions for G=0.5 shown in Fig. 10. Downstream of the hole centerlines effectiveness values close to unity are obtained at a position of x/d=3, whereas in-between the holes no cooling effect is visible. As mixing of

the jets occurs through the turbulent boundary layer, the effectiveness peaks gradually level out to a value of 0.2 at x/d=17.

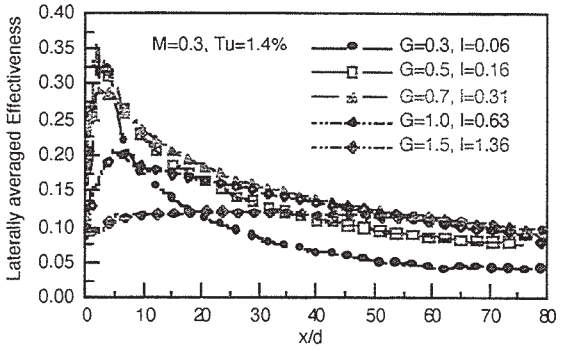

Figure 9 *Laterally averaged film cooling effectiveness on a flat plate*

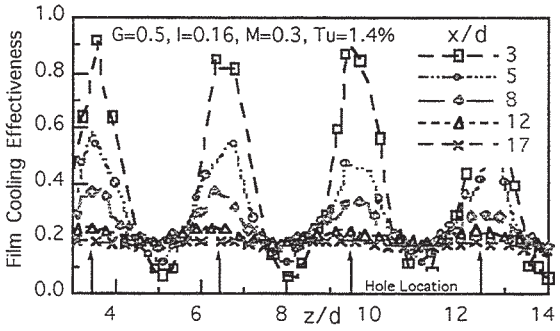

Figure 10 *Film cooling effectiveness on a flat plate at different axial positions*

Laterally averaged heat transfer augmentation with respect to an uncooled baseline test without cooling holes is presented in Fig. 11, for different blowing ratios at M=0.3. For all except the highest blowing ratio a remarkable increase in heat transfer is limited to about 10 hole diameters downstream of injection, whereafter it decreases to a value of 1. Only for the highest blowing ratio, a maximum of 20% increase occurs at x/d=20, which indicates the reattachment location of the jets after lift-off behind injection.

The spanwise distribution of heat transfer for G=0.5 is depicted in Fig. 12. The heat transfer is increased at locations where the edge of the jet and the mainstream interact. Such behavior was observed for all blowing ratios.

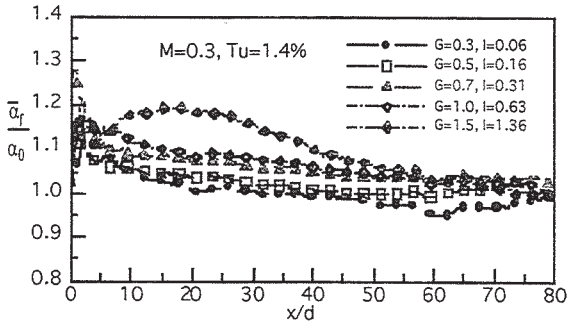

Figure 11 *Laterally averaged heat transfer augmentation on a film cooled flat plate*

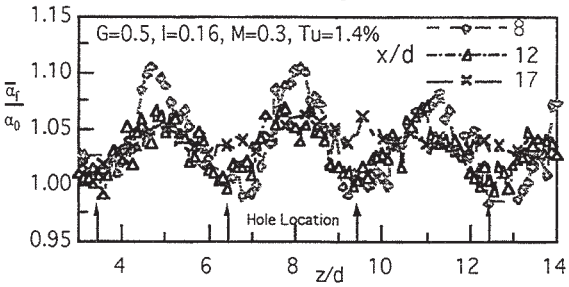

Figure 12 *Heat transfer augmentation on a film cooled flat plate at different axial positions*

Cylinder

Fig. 13 shows the evolution of $\overline{\eta}$ on the cylinder for different blowing ratios at a Mach number of 0.3. As on the flat plate jet lift-off occurs at blowing ratios exceeding 0.9 and highest overall effectiveness is observed at G=0.9.

The effect of the lateral hole inclination can be clearly seen from Fig. 14, where highest effectiveness values are laterally shifted in respect to the hole exit locations.

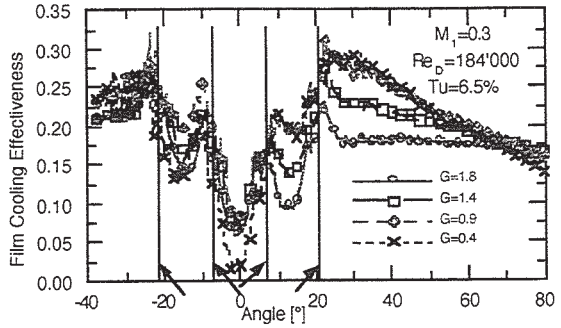

Figure 13 *Laterally averaged film cooling effectiveness on a cylinder*

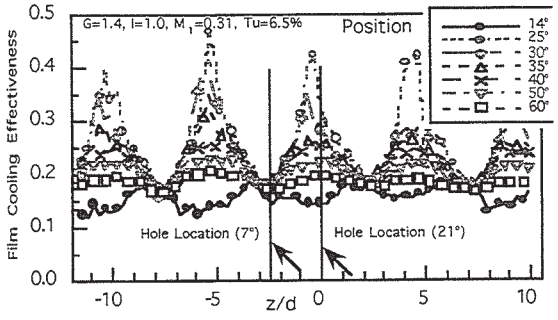

Figure 14 *Film cooling effectiveness on a cylinder at different axial positions*

Heat transfer in the presence of showerhead cooling is strongly increased due to important mixing of main and secondary flow (Fig. 15). Peaks as high as 3 in terms of $Nu/Re^{0.5}$ occur downstream of the injection locations, slightly decreasing with increasing blowing ratio.

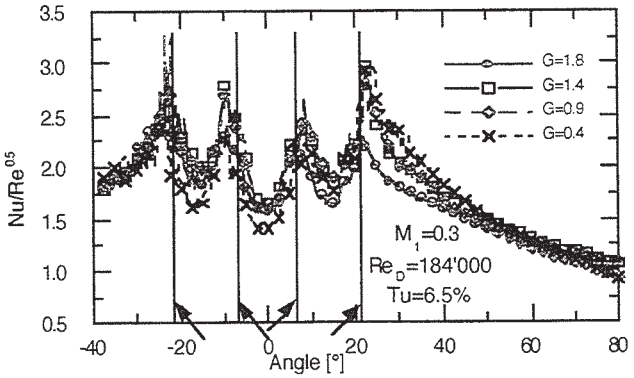

Figure 15 *Laterally averaged heat transfer on a cylinder*

CONCLUSIONS

The transient liquid crystal technique has been successfully used for film cooling measurements on a flat plate and a showerhead cooled cylinder. A multiple-test regression method has been developed for the data reduction, considering a transient coolant temperature evolution. This method allows the simultaneous deduction of the film cooling effectiveness and the heat transfer coefficients.

The utilization of this optical measurement technique permits to conduct complete surface measurements, which is especially important and usefull to reveal three-dimensional phenomena, as they occur in discrete hole film cooling.

ACKNOWLEDGMENTS

The research project is subsidized by ABB, Baden, Switzerland and the "Nationaler Energie-Forschungs Fonds" (NEFF), Switzerland.

REFERENCES

Baines, W.D. and Peterson, E.G., 1951
An Investigation of Flow through Screens.
ASME Transactions, Vol. 73, pp. 467-480

Häring, M., Hoffs, A., Bölcs, A., 1995
An Experimental Study to Compare the Naphthalene with the Liquid Crystal Technique in Compressible Flow
ASME Paper 95-GT-16

Teekaram, A.J.H., Forth, C.J.P., Jones, T.V., 1990
Film Cooling in the Presence of Mainstream Pressure Gradients
ASME Paper 90-GT-334

Vedula, R.,J., Metzger, D.E., 1991
A Method for the Simultanenous Determination of Local Effectiveness and Heat Transfer Distributions in Three-Temperature Convection Situations
ASME Paper 1991

Wang, Z., Ireland, P.T., Jones, T.V., 1994
A Colour Image Processing System for Transient Liquid Crystal Heat Transfer Experiments
ASME Paper 94-GT-290